

IAC-10-D4.4.5

THE EFFECT OF DISTURBANCES ON SPACE ELEVATOR DYNAMICS WITH FLEXIBILITY

Ryotaro. OhkawaNihon University, Japan, ryotarolab@yahoo.co.jp

Kenji Uchiyama

Nihon University, Japan, uchiyama@aero.cst.nihon-u.ac.jp

Hironori A. Fujii

Kanagawa Institute of Technology, Japan, fujii@tmit.ac.jp

A space elevator has been offered an alternate method for space transportation. With the discovery of carbon nanotube that has the strength-to-mass ratio required for the system, the construction of a space elevator has realistically been researched. The discussion of dynamical behaviour of the system is a necessity as well as the development of materials of the tether. We propose the fundamental model of a space elevator system to explore the underlying dynamics for design problems. The system consists of a very long tether with flexibility, a counterweight that is used to avoid too long tether, and an elevator ascending or descending along the tether. The length of the tether is longer than the geostationary altitude due to necessity of counterweight in equilibrium. The effect of elevator transit on the motion of the flexible tether is considered as a disturbance. In this paper the equations of its motion which takes flexibility of the tether and the motion of the elevator into account are formulated as a distributed parameter system. The longitudinal vibration of the tether is ignored in its dynamics since the frequency of the mode is very high in comparison with the lateral vibration of the tether. In the numerical simulation Crank-Nicolson method is applied to the equation to calculate stably the dynamics of the system.

NOMENCLATURE

A	=	cross-sectional area of the tether
C	=	period of natural frequency of the tether assuming a uniform chord
\mathbf{F}_e	=	force vector caused by elevator motion
L	=	length of the tether
M	=	mass of the tether
m_c	=	mass of the counterweight
m_e	=	mass of the elevator
m_s	=	mass of a segment of the tether
R_E	=	radius of the Earth
ℓ	=	length of a tether segment
\mathbf{r}	=	position vector at of a tether segment
\mathbf{r}_e	=	position vector of the elevator
\mathbf{r}_0	=	position vector at the end of the tether which coincides with the origin of moving coordinate system
\mathbf{r}_f	=	position vector of another end of the tether
\mathbf{T}	=	tension vector
θ	=	angle between tension at a tether segment and x axis
ρ	=	density of the tether
μ_E	=	gravitational constant of the Earth
Ω	=	spin rate of the Earth

Subscript

x	=	component of a vector along x axis
y	=	component of a vector along y axis

I. INTRODUCTION

A space elevator which consists of a long tether stretching from the Earth's surface to beyond geostationary altitude has been considered as one of useful space transportation systems and discussed by many researchers over number of years. The concept of the space elevator was proposed for the first time by K. E. Tsiolkovsky¹ in the late of nineteenth century. In 1960's, Y. N. Astdutanov² presented the idea of the space elevator more specifically. After that, J. Person³ proposed the method of construction and designed the configuration of the tether. However, the space elevator was not studied until later because there was no material to match the condition to afford the strength especially tension of material to construct it. In the 1990's the discovery of the carbon nanotube that possesses high-intensity makes the space elevator system feasible. Then its dynamics has been analyzed using simple model by many researcher⁵⁻⁹. P. Williams^{10,11} analyzed vibration of the tether using the dynamic model based on a lumped mass approximation. There are several studies¹²⁻¹⁸ concerning the system, however, the dynamics has not been sufficiently clarified in realistic model.

Generally, the model of the space elevator system is formulated using the lumped mass approach, i.e. the tether is divided into a large number of discrete masses that are connected by viscoelastic springs. If the tether is assumed to be a chord, the lumped mass model is not appropriate.

In this paper, the dynamic model is formulated for the space elevator system that consists of a tether with flexibility, a counterweight and an elevator. Firstly, we propose its dynamic model expressed by the distributed parameter system. The dynamic behaviour is analyzed numerically by using Crank-Nicolson method.

II. SYSTEM DESCRIPTION

II.1 Counter weight

Figure 1 shows the schematic representation of the physical model of the space elevator system. The Earth is assumed to be completely sphere. The x - y axis denotes the moving coordinate system whose origin agrees with the centre of the Earth. The anchor point of the tether is located on the surface of the Earth. The direction of the x axis is determined to be from the centre of the Earth to the anchor point. Therefore, angular velocity of the rotating coordinate system is equal to the spin rate of the Earth, Ω . The elevator can ascend or descend along the flexible tether with constant speed. A counterweight is treated to avoid too long tether shown in the figure.

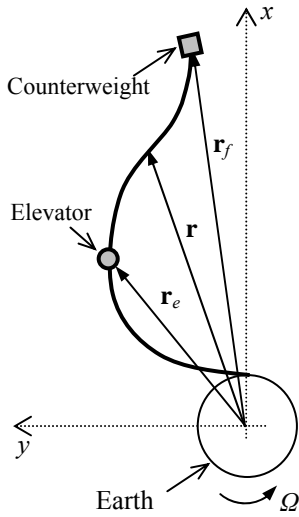


Fig.1: Physical model of space elevator system which consists of tether, counterweight, and elevator

It is necessary for the system to keep the balance of force acting on the tether. In the case of the system without an elevator the condition for the necessity was obtained by the following equation⁴.

$$\int_0^{r_f} \rho A (x\Omega^2 - \frac{\mu_E}{x^2}) dr = 0 \quad [1]$$

The tether length is found to be about 150,000km in Ref.4. In this paper, a counterweight attached at the end of the tether as shown in Fig.1 is employed to avoid such the very long tether system. The basic concept of

the system with counterweight was proposed by Clarke³. According to the necessity for the system should satisfy the following condition.

$$\rho A \int_0^L (x\Omega^2 - \frac{\mu_E}{x^2}) dx + m_c (L\Omega^2 - \frac{\mu_E}{L^2}) = 0 \quad [2]$$

It is noted that the force balance only along x axis is considered to keep the equilibrium state of the system. The density and the cross-sectional area of the tether are assumed to be constant. It is supposed that the displacement caused by lateral vibration of the flexible tether is sufficiently small in comparison with its length i.e. the integral interval can be treated as shown in Eq.[2].

The mass of the counterweight can be calculated by Eq.[2]. Strictly speaking, it is difficult to satisfy Eq.[2] because the vibration of the tether and the mass of the elevator are ignored in the condition. If the equation for the force balance is not satisfied, the system falls to the Earth. For this reason, it is suggested that the following inequality is used when calculating the mass of the counterweight.

$$\rho A \int_0^L (x\Omega^2 - \frac{\mu_E}{x^2}) dx + m_c (L\Omega^2 - \frac{\mu_E}{L^2}) > 0 \quad [3]$$

The mass of the counterweight depends upon the tether's cross-sectional area and the length of the tether without flexibility. Figure 2 shows the results of the calculation.

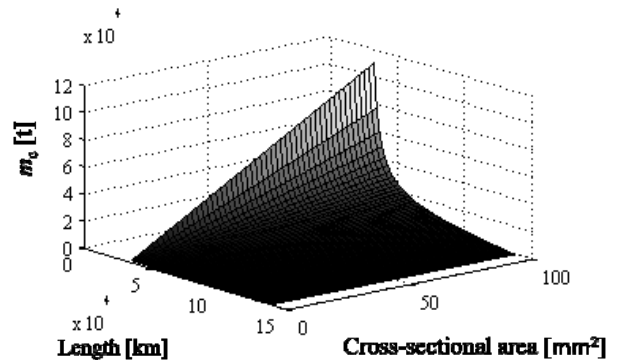


Fig.2: Mass of counterweight corresponding to cross-sectional area and total length of tether

II. II Dynamics

Figure 3 shows a tether segment model. The vector of the tension at the tether segment with a length of ℓ can be broken down into the components along x and y direction.

$$\begin{aligned} T_x &= \cos \theta \cdot dT - T \sin \theta \cdot d\theta \\ T_y &= \sin \theta \cdot dT + T \cos \theta \cdot d\theta \end{aligned} \quad [4]$$

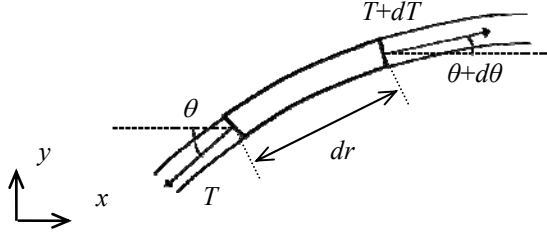


Fig.3: Tension at tether segment

The changes of the tension and the angle, dT and $d\theta$, respectively, are very small in the tether segment. Assuming the angle θ is less than one degree, the equations can be easily linearized by using $\cos\theta \approx 1$, $\sin\theta \approx \theta$.

The elevator moves with constant velocity v_e on the flexible tether from the surface of the Earth to the geostationary orbit (see Fig.4). The elevator is assumed to be a particle. The counterweight is set up at the end of the tether shown in Fig.4 and another end of the tether is firmly fixed on the surface of the Earth. Although the flexible tether is treated in the analysis, the longitudinal vibration is not considered.

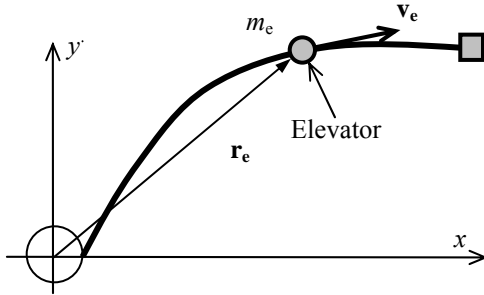


Fig.4: Model of space elevator moving on tether

The relative motion of the tether segment can be written as

$$m_s \frac{d^2 \mathbf{r}}{dt^2} = m_s \left(\Omega^2 - \frac{\mu_E}{r^3} \right) \mathbf{r} + \mathbf{T} + \mathbf{F}_e \delta(\mathbf{r} - \mathbf{r}_e) \quad [5]$$

where δ denotes Dirac delta function. The motion of the elevator is free from friction between the elevator and the tether. The Coriolis force is not considered here because the velocity of the tether segment in x direction will not too fast¹⁹.

As mentioned previously, the angle θ is assumed to be sufficiently smaller than one degree. Then $\sin \theta \approx \theta \approx \partial y / \partial x$, and $r \approx x$. Substituting Eq.[4] into Eq.[5], the linearized equations of motion of the tether system can be obtained.

$$\rho A \left(\Omega^2 x - \frac{\mu_E}{x^2} \right) + \frac{\partial T}{\partial x} + \frac{F_{ex}}{\ell} = \rho A \frac{\partial^2 x}{\partial t^2} \quad [6]$$

$$T \frac{\partial^2 y}{\partial x^2} + \frac{\partial T}{\partial x} \frac{\partial y}{\partial x} + \rho A \left(\Omega^2 - \frac{\mu_E}{x^3} \right) y + \frac{F_{ey}}{\ell} = \rho A \frac{\partial^2 y}{\partial t^2} \quad [7]$$

II. III Tension

The tension of the tether is calculated here in static balance to verify the stress of the tether, i.e. the acceleration and velocity of the tether in Eq.[6] is assumed to be zero and \mathbf{F}_e is not considered. Then the following equation in terms of the tension of the tether segment is derived.

$$dT = \rho A (\mu_E x^{-2} - \Omega^2 x) dx \quad [8]$$

If the counterweight is located at end of the tether, the tensile strength at a segment of the tether is expressed as follows:

$$T(x) = \int_x^L \rho A (\mu_E x^{-2} - \Omega^2 x) dx + m_c \left(\frac{\mu_E}{L^2} - \Omega^2 L \right) \quad [9]$$

Figure 5 shows relationship between the stress and length of the tether. In the case of no counterweight the total length of the tether becomes 144,630 km to keep the force balance⁴. The length of the tether with the counterweight is set to be 40,000 km that is longer than the altitude of the geostationary orbit.

It is slightly recognized from the figure that the maximum stress of the latter case is less than the very long tether. The result of calculation shows that tensile strength of the material requires more than 18 GPa. Therefore, there is possibility of the realization of the space elevator system with the counterweight because the maximum tensile strength of carbon nanotube which is considered for one of the material of tether will be about 65 GPa²⁰⁻²².

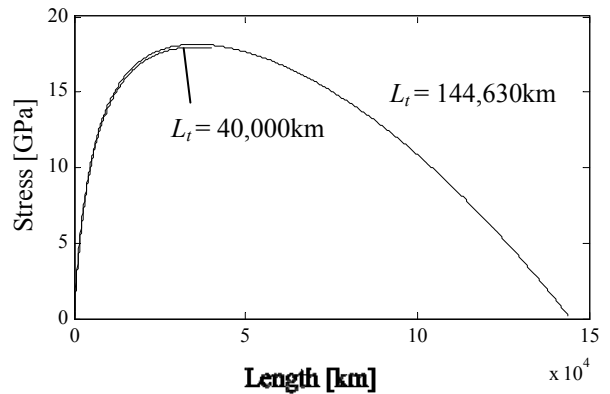


Fig.5: Plot of stress of tether versus length of tether

III. NUMERICAL SIMULATION

III.I Descretization

In this section, the equation of motion of the tether expressed by Eq.[5] is transformed into a difference equation for numerical simulation by using Crank-Nicolson method²³ because there is a condition concerning Δt and Δx to decide those values.

$$\begin{aligned}
 & -\frac{T\Delta t^2}{2m_s\Delta x^2}y_{k+1}^{t+1} + \left(\frac{T\Delta t^2}{m_s\Delta x^2} + 1\right)y_k^{t+1} - \frac{T\Delta t^2}{2m_s\Delta x^2}y_{k-1}^{t+1} \\
 & = \frac{\Delta t^2}{2m_s} \left(\frac{T}{\Delta x^2} + \frac{f_1}{\Delta x} \right) y_{k+1}^t \\
 & + \left(-\frac{T\Delta t^2}{m_s\Delta x^2} + \frac{f_2\Delta t^2}{m_s} + 2 \right) y_k^t \\
 & - \frac{\Delta t^2}{2m_s} \left(\frac{T}{\Delta x^2} - \frac{f_1}{\Delta x} \right) y_{k-1}^t - y_k^{t-1} + \frac{\Delta t^2}{m_s} \frac{F_{ey}}{\ell}
 \end{aligned} \quad [10]$$

where

$$\begin{aligned}
 f_1 & = \frac{\partial T}{\partial x} \\
 f_2 & = \rho A \left(\Omega^2 - \frac{\mu_E}{x^3} \right)
 \end{aligned}$$

The end of the flexible tether is fixed on the surface of the Earth and another end is free. The following conditions expressed by difference equations are derived to satisfy the boundary conditions of the tether.

$$\begin{aligned}
 y_k^{t+1} & = \frac{T}{m_s} \frac{\Delta t^2}{\Delta x^2} y_{k+2}^t + \frac{\Delta t^2}{m_s} \left(-2\frac{T}{\Delta x^2} + \frac{f_1}{\Delta x} \right) y_{k+1}^t \\
 & + \left(\frac{T\Delta t^2}{m_s\Delta x^2} - \frac{f_1\Delta t^2}{m_s} + f_2 + 2 \right) y_k^t - y_k^{t-1} + \frac{\Delta t^2}{m_s} \frac{F_{ey}}{\ell}
 \end{aligned} \quad [11]$$

and

$$\begin{aligned}
 y_k^{t+1} & = \frac{T}{m_s} \frac{\Delta t^2}{\Delta x^2} y_{k-2}^t + \frac{\Delta t^2}{m_s} \left(-2\frac{T}{\Delta x^2} - \frac{f_1}{\Delta x} \right) y_{k-1}^t \\
 & + \left(\frac{T\Delta t^2}{m_s\Delta x^2} + \frac{f_2\Delta t^2}{m_s} + f_2 + 2 \right) y_k^t - y_k^{t-1} + \frac{\Delta t^2}{m_s} \frac{F_{ey}}{\ell}
 \end{aligned} \quad [12]$$

III. II Free vibration

Both cases of 40,000 km length with a counterweight and 144,630 km length without a counterweight are simulated in this calculation. Disturbances such as the elevator motion, solar pressure, and J_2 term are not taken into account for the analysis of the space elevator system. Other parameters are set as shown in Table 1. The mass of the counterweight is calculated by Eq.[3].

Table 1. Parameter for numerical simulation

Parameter	Value
Tether length (km)	40,000
Counter weight mass (ton)	1,112
Elevator mass (kg)	1000
Density of tether (kg/m ³)	1400
Cross-sectional area of tether (mm ²)	1
Elevator speed (km/h)	300

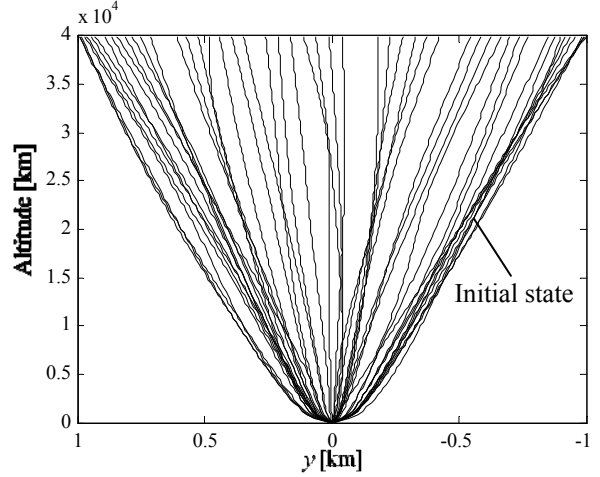


Fig.6: Dynamic behaviour of flexible tether with counterweight

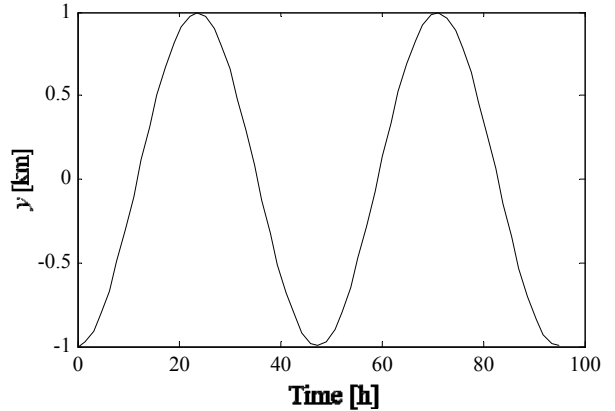


Fig.7: Time response of flexible tether with counterweight at free end

Figures 6 and 7 show the results with respect to the shorter tether with 40,000 km length. The first mode of the flexible tether is appeared under this condition as shown in Fig.6. Figure 7 shows the time response of the displacement at the free end of the tether. The time period of this mode is 47.7 hrs. The time period agrees with the calculation result using an analytical solution for a string with some assumptions. Higher mode of vibration of the system does not occur due to the counterweight.

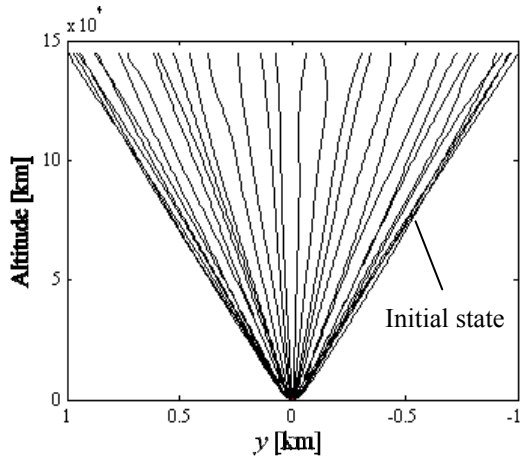


Fig.8: Dynamic behaviour of very long tether without counterweight

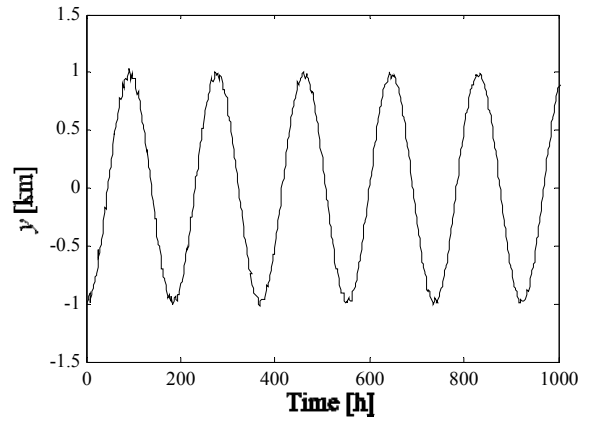


Fig.9: Time response of very long tether without counterweight at free end

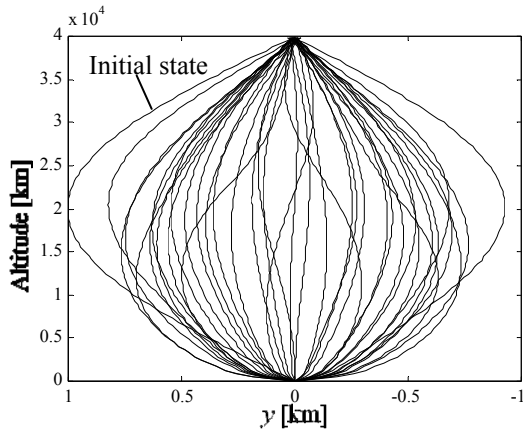


Fig.10: Dynamic behaviour of flexible tether with counterweight (initial shape is sinusoidal wave)

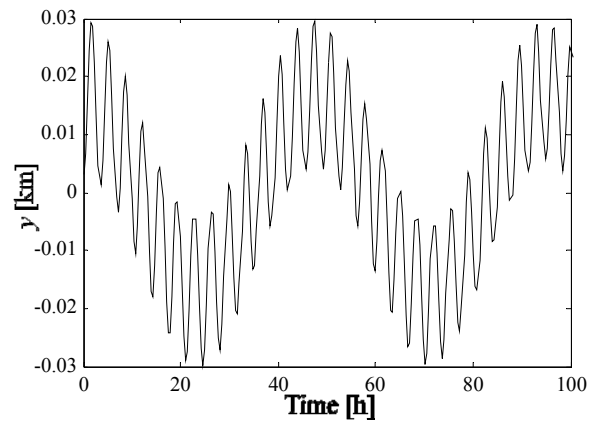


Fig.11: Time response of tether with counterweight (initial shape is sinusoidal wave)

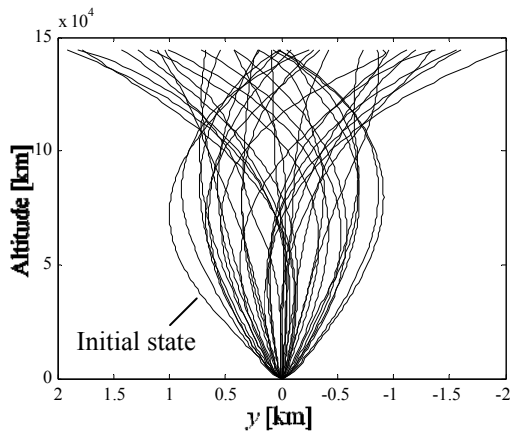


Fig.12: Dynamic behaviour of flexible tether without counterweight (initial shape is sinusoidal wave)

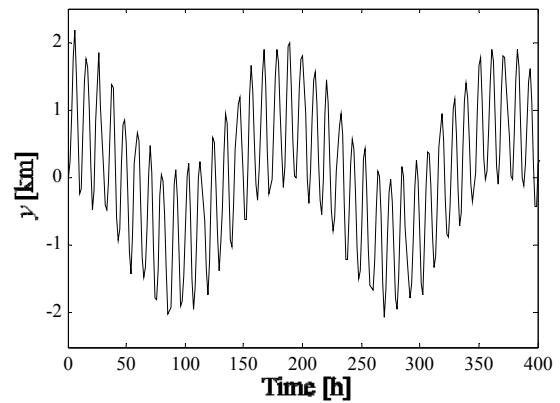


Fig.13: Time response of tether without counterweight at free end (initial shape is sinusoidal wave)

Figures 8 and 9 show dynamic behaviour of the longer tether with 144,630 km length. It is clear from Fig.9 that the second mode of the tether can be recognized. The time periods of first and second modes are 189 hrs and 12 hrs, respectively.

Figures 10 to 13 shows dynamic behaviour of the flexible tether. Initial shape of the tether is set to be sinusoidal wave. In the case of using counterweight, the second mode of the tether occurs under the initial condition. The time periods of the modes are 47.7 hrs and 3.52 hrs as shown in Fig. 11.

Figure 12 shows the dynamic behaviour of the space elevator system without the counterweight. The displacement of the tether at free end is larger than the case of using the counterweight. It is shown from Fig 13 that the time period of the flexible tether is larger than the previous case.

III. III Effect of elevator motion

The values of parameter such as elevator weight are used shown in Table 1. The elevator ascends or descends with constant speed along the flexible tether between the surface of the Earth and the geostationary orbit.

Figure 14 shows the dynamic behaviour of the system with the elevator ascending at constant speed 300km/h along the tether with a 40,000 km length. Initial shape of the tether is assumed to be straight line in this simulation. The black particle in Fig.14 denotes the elevator. When ascending along the tether, the elevator moves right direction at the beginning of the numerical simulation due to the Coriolis force as shown this figure. The elevator reaches the geostationary orbit after about 120 hrs.

Figure 15 shows the dynamic behaviour of the space elevator system after the elevator reaches the geostationary orbit. The time response of the tether at the free end is shown in Fig.16. It should be noted that the effect of the elevator motion on the dynamic behaviour of the tether can not be ignored during ascent of the elevator. The amplitude of the vibration after ascent of the elevator is about 200 m in this case. It should be noted that a method would be necessary to keep stability of the system even though the amplitude is sufficiently small in comparison with the length of the tether.

Figures 17 to 19 show the results of numerical simulation in the case of descent of the elevator with constant speed 300 km/h from the geostationary orbit to the surface of the Earth. At the beginning of the numerical simulation the Coriolis force acts on the flexible tether in left direction as shown in Fig.17. Higher modes of the tether are excited during descent of the elevator.

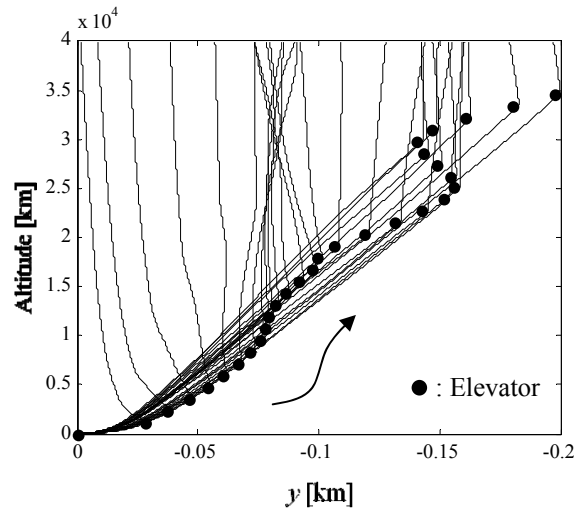


Fig.14: The effect of elevator ascending at 300km/h along 40,000km tethered system

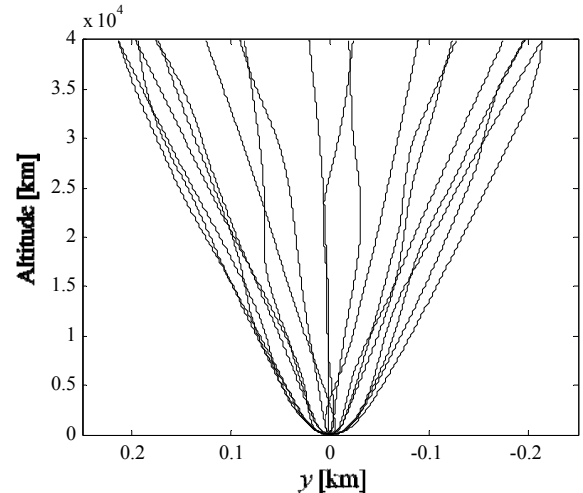


Fig.15: Dynamic behaviour of space elevator system after elevator reaches geostationary orbit

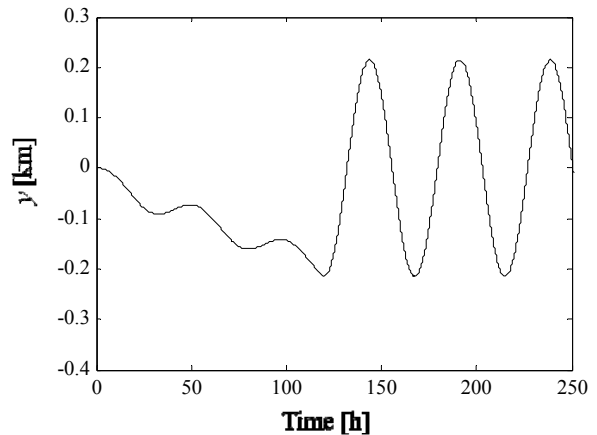


Fig. 16: Time response of tether at free end

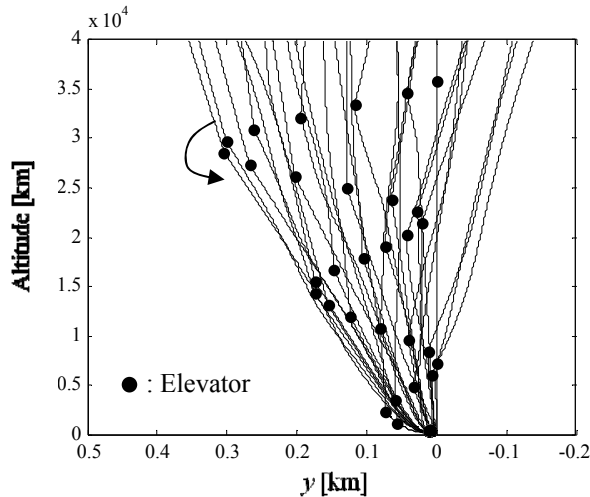


Fig.17: Effect of elevator motion on flexible tether during descent

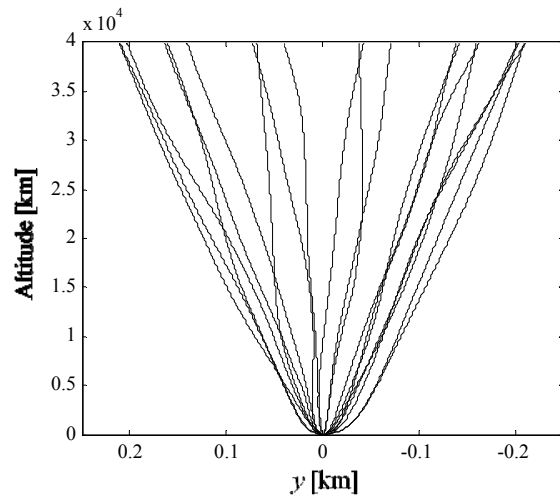


Fig.18: Vibration of flexible tether after elevator reaches surface of the Earth

IV. CONCLUSION

In this paper, we formulated the equations of motion of the space elevator system considering the motion of the elevator. The system consists of a flexible tether, an elevator, and a counterweight to avoid too long tether.

The inequality was proposed to calculate the mass of the counterweight to keep the stability of the system. The length of tether is 40,000 km and the mass of the counterweight is calculated as 1,112 ton for the proposed space elevator system. The Coriolis force acts on the flexible tether during ascent and descent of the elevator with constant speed. The motion of the elevator excites lower modes of the flexible tether.

The optimal profile with respect to the speed of the space elevator should be considered to suppress the vibration of the flexible tether.

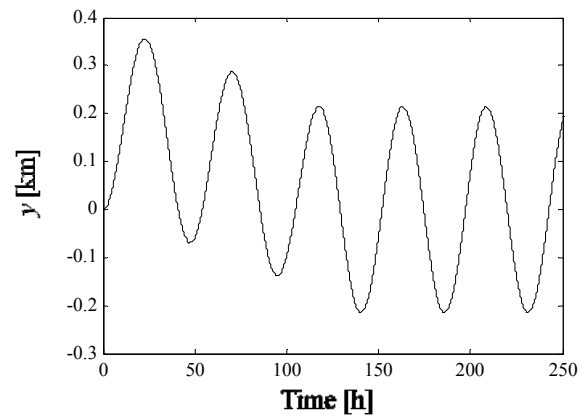


Fig.19: Time response of flexible tether during and after descent

¹ K. E. Tsiolkovsky, *Speculations between Earth and sky*, Isd-vo AN-SSSR, Moscow, 1895, p.35

² Y.N. Artsutanov, *To space by a locomotive*, Komsomolskaya Pravda, 1960

³ A. C. Clarke., *The Space Elevator: 'thought experiment', or key to the universe*. *Advances in Earth Oriented Applied Science Technology*, 1979,1, 39.

⁴ J. Pearson, *The orbital tower: a spacecraft launcher using the Earth's rotational energy*, *Acta Astronautica Vol.2*, 1975, pp.785-799

⁵ B.C. Edwards and E. A. Westling, *The Space Elevator: A Revolutionary Earth-to-Space Transportation System*, 2003.

⁶ B.C. Edwards, *Design and Deployment of a Space Elevator*, *Acta Astronautica Vol.47*, 2000, pp.735-744

⁷ P. Ragan, B. C. Edwards, *Leaving the Planet by Space Elevator*, lulu. Com, 2009

⁸ C. R. McInnes, *Dynamics of a Particle Moving Along an Orbital Tower*, *Journal of Guidance, Control and Dynamics*, vol. 28, No. 2, 2005

⁹ C. R. McInnes and C. Davis, *Novel Payload Dynamics on Space Elevators System*, 56th International Astronautical Congress, Fukuoka, 2005, IAC-05-D4.2.07

-
- ¹⁰P. Williams, Wubbo Ockels, Climer Motion Optimization for the tether Space Elevator, AIAA/AAS Astrodynamics Specialist Conference and Exhibit, 18-21 August, 2008, AIAA 2008-7383
- ¹¹P. Williams, Dynamic Multibody Modeling for Tethered Space Elevators, *Acta Astronautica* Vol. 65, 2009, pp.399-422
- ¹²Stephen S. Cohen, Arun K. Misra, Elastic Oscillations of the Space Elevator Ribbon, *Journal of Guidance, Control, and Dynamics*, Vol. 30, No. 6, 2007, pp.1711-1717
- ¹³Stephen S. Cohen, Arun K. Misra, The Effect of Climber Transit on the Space Elevator Dynamics, *Acta Astronautica* 64, 2009, pp.538-553
- ¹⁴Lang, D. D., Space Elevator Dynamic Response to In-Transit Climbers, 1st International Conference on Science, Engineering, and Habitation in Space, Albuquerque, NM, Space Engineering and Science Inst., 2006, Paper 10152148
- ¹⁵N. Pugno, M. Schwarzbart, A. Steindl, H. Troger, On the Stability of the Track of the Space Elevator, *Acta Astronautica* Vol.64, 2009, pp.524-537
- ¹⁶Pamela Woo, Arun K. Misra, Dynamics of a Partial Elevator with Multiple Climbers, *Acta Astronautica*, Vol.67, 2010, pp.753-763
- ¹⁷E. C. Lorenzini, M. Cosmo, Wave progration in the tether elevator/Crawler system, *Acta Astronautica* Vol. 21, No. 8, 1990, pp. 545-552
- ¹⁸H. A. Fujii, M. Ohta, T. Watanabe, T. Ogasawara, Study of Feasibility and Characteristic of Space Elevator, 25th International Symposium on Space Technology and Science (Selected Paper), 2006, 2006-g-07
- ¹⁹K. Satoh, H. A. Fujii, K. Iijima, R. Ohkawa, K. Uchiyama, Study on Fundamental Dynamics of Very Long Tether System, the 5th Asian Conference on Multibody Dynamics, 2010.
- ²⁰H. Peng, D. Chen, J. Y. Huang, et al., Strong and Ductile Colossal Carbon Tubes with Walls of Rectangular Macropores, *Phys. Rev. Lett.* 101 (14): 145501
- ²¹Yu, Min-Feng, Strength and Breaking Mechanism of Multiwalled Carbon Nanotubes Under Tensile Load, *Science* 287 (5453), pp.637-640
- ²²K. Hata, From Highly Efficient Impurity-Free CNT Synthesis to DWNT forests, CNTsolids and Super-Capacitors
- ²³J. Crank and P. Nicolson, Practical Method for Numerical Evaluation of Solutions of Partial Differential Equations of the Heat-Conduction Type, *Advances in Computational Mathematics* 6, 1996, pp.207-226